Photoinduced Long-Lived Charge Separation in a Tetrathiafulvalene−Porphyrin−Fullerene Triad Detected by Time-Resolved Electron Paramagnetic Resonance

ARTICLE *in* THE JOURNAL OF PHYSICAL CHEMISTRY B · AUGUST 2005

Impact Factor: 3.3 · DOI: 10.1021/jp051345c · Source: PubMed

Photoinduced Long-Lived Charge Separation in a Tetrathiafulvalene−Porphyrin−Fullerene Triad Detected by Time-Resolved Electron Paramagnetic Resonance

Marilena Di Valentin,[†] Arianna Bisol,[†] Giancarlo Agostini,[‡] Paul A. Liddell,[§] Gerdenis Kodis,[§] Ana L. Moore,[§] Thomas A. Moore,[§] Devens Gust,[§] and Donatella Carbonera*[,†]

Dipartimento di Scienze Chimiche, Università di Padova, via Marzolo 1, I-35131 Padova, Italy, CNR—Istituto di Chimica Biomolecolare, Sezione di Padova, via Marzolo 1, I-35131 Padova, Italy, and Center for the Study of Early Events in Photosynthesis, Department of Chemistry and Biochemistry, Arizona State University, Tempe, Arizona 85287-1604

Received: March 15, 2005; In Final Form: May 12, 2005

Photoinduced electron transfer has been observed in a molecular triad, consisting of a porphyrin (P) covalently linked to a tetrathiafulvalene (TTF) and a fullerene derivative (C_{60}), in the different phases of the liquid crystal E−7 and in a glass of 2-methyltetrahydrofuran (2-MeTHF) by means of time-resolved electron paramagnetic resonance (EPR) spectroscopy. In both solvents, an EPR signal observed immediately after excitation has been assigned to the radical pair $TTF^{\bullet+}-P-C_{60}^{\bullet-}$, based on its magnetic interaction parameters and spin polarization pattern. In the 2-MeTHF glass and the crystalline phase of E−7, the $TTF^{\bullet+}-P-C_{60}^{\bullet-}$ state is formed from the $TTF-{}^1P-C_{60}$ singlet state via an initial $TTF-P^{\bullet+}-C_{60}^{\bullet-}$ charge-separated state. Long-lived charge separation ($\sim$8 μs) for the singlet-born radical pair is observed in the 2-MeTHF glass at cryogenic temperatures. In the nematic phase of E−7, a high degree of ordering in the liquid crystal is achieved by the molecular triad. In this phase, both singlet- and triplet-initiated electron transfer routes are concurrently active. At room temperature in the presence of the external magnetic field, the triplet-born radical pair $^T(TTF^{\bullet+}-P-C_{60}^{\bullet-})$ has a lifetime of $\sim$7 μs, while that of the singlet-born radical pair $^S(TTF^{\bullet+}-P-C_{60}^{\bullet-})$ is much shorter ($<$1 μs). The difference in lifetimes is ascribed to spin dynamic effects in the magnetic field.

Introduction

Porphyrin-based covalently linked ensembles of electron donor and acceptor moieties have long been investigated as models for the photoinduced electron-transfer process characteristic of photosynthesis.[1−7] More recently, it has been found that fullerene derivatives have many properties that make them excellent electron acceptor components of such supramolecular systems. Functionalized fullerene molecules are characterized by first reduction potentials similar to those of quinones, which are naturally occurring redox couples. They have small internal and solvent reorganization energies and low sensitivity to solvent stabilization of their anions.[8−11] These features all together lead to rapid photoinduced electron transfer (ET) and slow charge recombination. Since the first report of photoinduced ET in a molecular dyad consisting of a fullerene derivative covalently linked to a porphyrin,[12] fullerenes have been incorporated in many molecular dyads and triads that act as artificial reaction centers.[13−15] Among these molecular devices, the carotenoid (C), porphyrin (P), and fullerene (C_{60}) molecular triads, which have been extensively investigated by both optical and magnetic time-resolved spectroscopies, have shown interesting properties as model compounds for photosythesis.[9,16−22] Molecular triads of this general type mimic several aspects of photosynthetic ET, including photoinduced ET in glasses at low temperatures, charge recombination to yield the carotenoid triplet state rather than the molecular ground state, and photoprotection from singlet oxygen generation by a thermally activated triplet energy transfer relay mechanism.[19]

Although charge recombination to give triplet states, which is found only in a few model systems, reproduces the recombination process between the primary donor and an electron acceptor occurring in natural photosynthetic reaction centers after prereduction or removal of secondary acceptors,[23,24] it also limits the lifetime of charge separation,[9] and this can make it more difficult to couple the charge separation to succeeding electronic processes. A solution to this problem is to employ electron donors and acceptors whose triplet energies lie above those of the relevant charge-separated states.

Tetrathiafulvalene is a well-known electron donor that has been paired with fullerenes in a variety of molecular dyads and triads[25−33] and whose lowest triplet state lies at a significantly higher energy than that of carotenes.[34,35] Molecular triad **1** (Chart 1), which contains a porphyrin chromophore (P) covalently linked to a fullerene electron acceptor (C_{60}) and a tetrathiafulvalene electron donor (TTF) has been recently reported.[36,37] Transient optical spectroscopy studies[36] demonstrated that excitation of the porphyrin moiety in a 2-methyltetrahydrofuran (2-MeTHF) solution at ambient temperature yields the porphyrin first excited singlet state $TTF-{}^1P-C_{60}$, which undergoes photoinduced electron transfer with a time constant of 25 ps to give $TTF-P^{\bullet+}-C_{60}^{\bullet-}$. This intermediate charge-separated state has a lifetime of 230 ps, decaying mainly by charge shift to give the final charge-separated state $TTF^{\bullet+}-P-C_{60}^{\bullet-}$. This state is formed with a yield of 92% and decays to the ground state in 660 ns. The relevant transient states of triad **1** are illustrated in Figure 1.

* Author to whom correspondence should be addressed. Phone: +39-049-827-5144. Fax: +39-049-827-5161. E-mail: donatella.carbonera@unipd.it.

[†] Università di Padova.

[‡] CNR—Istituto di Chimica Biomolecolare.

[§] Arizona State University.

10.1021/jp051345c CCC: $30.25
Published on Web 07/12/2005

CHART 1: Structure of Triad 1 and Related Model Compounds 2 and 3

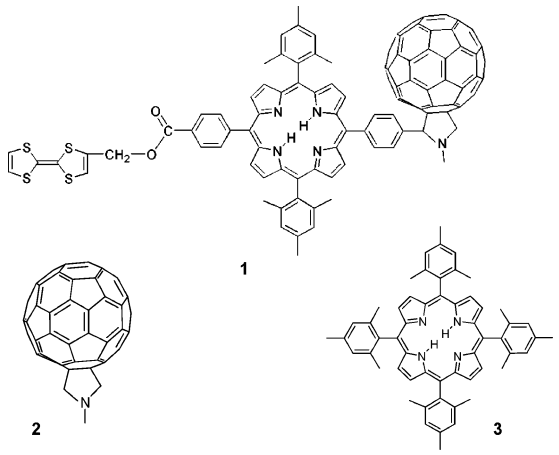

As a further step in the mimicry of the photosynthetic process, artificial molecular systems have been embedded in liquid crystals[3,38,39] or inserted into the membranes of liposomes[6,40−42] to model the natural anisotropic media (proteins in membranes). For example, a carotenoid−porphyrin−quinone molecular triad, inserted in liposomes, has been able to harvest light energy and drive the production of proton motive force and ATP.[41]

Time-resolved electron paramagnetic resonance (TREPR) spectroscopy is unique in revealing details of the electron-transfer process. Spin polarization can be used to elucidate the mechanisms of formation of spin-correlated radical pairs and triplet states resulting from electron transfer.[43] Liquid crystals are, for many reasons, convenient media for time-resolved electron spin resonance studies of these states.[38,39] TREPR investigations of intramolecular electron transfer in covalently linked donor−acceptor systems embedded in liquid crystals have shown that ET rates may be reduced by orders of magnitude due to the nematic potential associated with the alignment of the liquid crystal molecules, which, in turn, restricts the reorientational motion of the molecules undergoing ET. This effect has been exploited to make possible the detection on the time scale of TREPR of various species involved in ET.[39,44−46] Paramagnetic species can be detected in the crystalline and in the fluid nematic phases over a wide temperature range, allowing fine-tuning of the reorganization energy and of the energy levels of the charge-separated states.[45−49] The advantages of using liquid crystals include both improved kinetic information and improved spectral information. The anisotropy imposed by the nematic potential on the guest molecules introduces orientational effects on the spectra, which can be used to derive the magnetic interaction parameters, including the exchange interaction J between the two interacting spins. The value of J provides a measure of the electronic coupling for ET reactions.[50−53]

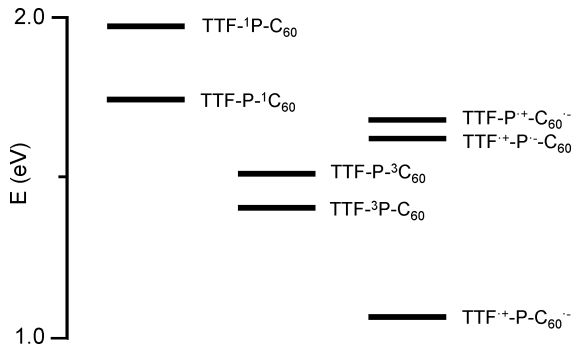

Figure 1. Energies of relevant transient states for triad **1**. The energies of the various states have been estimated from spectroscopic and cyclic voltammetric data obtained in polar solvents.[36]

In this work, the investigation of the charge separation and charge recombination processes for molecular triad **1**, previously reported in the relatively polar isotropic solvent 2-MeTHF at room temperature,[36] has been extended to the glass of 2-MeTHF and to the different phases of the liquid crystal (LC) E−7 using TREPR spectroscopy.

Experimental Section

Time-resolved EPR spectra were obtained using an apparatus that featured pulsed laser light guided into an X-band EPR spectrometer (Bruker ECS106) equipped with a TE_{102} cavity (9.4 GHz) and a nitrogen flow system. For measurements at cryogenic temperatures, an Oxford helium cryostat (ESR 200) was used. The time resolution of the TREPR spectrometer was ∼200 ns. Laser excitation at 532 nm (10 mJ per pulse and repetition rate of 10 Hz) was provided by the second harmonic of a Nd:YAG laser (Quantel Brilliant). Excitation at this wavelength yields mostly C−^{1}P−C_{60}. The microwave power used for the TREPR experiments was about 20 mW at the cavity. No field modulation or phase-sensitive detection was used. The EPR signals were taken from the microwave preamplifier (ER047-PH Bruker, bandwidth 20 Hz−6.5 MHz) and sampled with a LeCroy LT364 oscilloscope (1 ns per point). To eliminate the laser background signal, transients were accumulated under off-resonance field conditions and subtracted from those on resonance. The spectra at different times after the laser pulse were reconstructed from kinetic traces for each field position.

The synthesis of triad **1** has been reported elsewhere.[36] The TREPR experiments were performed on the molecular triad either dissolved in purified 2-MeTHF (Sigma-Aldrich) or embedded and oriented in the liquid crystal E−7 (Merck). E−7 is characterized by a positive diamagnetic susceptibility $\Delta\chi$, dielectric constants $\epsilon_{||} = 19.6$ and $\epsilon_{\perp} = 6.2$, and the following phase transition temperatures: crystalline ← 210 K → soft glass ← 263 K → nematic ←333 K → isotropic.

The LC samples (∼1×10^{-4} M) were prepared by dissolving triad **1** in toluene solution, evaporating the solvent to form a film of **1**, and then introducing E−7. The 2-MeTHF samples (∼4×10^{-4} M) were prepared by dissolving **1** directly in the solvent. All the samples were deaerated by several freeze−thaw cycles and sealed under vacuum. TREPR experiments were performed on samples at different concentrations to rule out intermolecular processes or aggregation effects.

The alignment of the liquid crystal samples was carried out by exposing the nematic phase to an external high magnetic field (6000 G) for 10 min at ambient temperature and then cooling to the required temperature.[54] In the fluid nematic phase of E−7, the director **L** is aligned parallel to the external magnetic field **B**. In the crystalline phase, different sample orientations, in terms of **L** with respect to the magnetic field, were investigated; **L** || **B** is the default orientation caused by the alignment, and the other orientations were reached by turning the EPR tube, mounted on a goniometer, in the cavity about an axis perpendicular to the external magnetic field.

Molecular modeling was performed in CS *Chem3D* (MM2) to obtain the optimized ground-state geometry of the triad. The extended conformation, which is employed in the graphical representation of Figure 4, corresponds to a minimum of energy, and it is also compatible with the TREPR results, as discussed below. However, a variety of distorted conformations are also possible with slightly higher energies.

TREPR Spectra Simulations. The spin-correlated radical pair spectral analysis was performed using programs in the MATLAB language kindly provided by Dr. M. Fuhs, from the Freie Universität of Berlin, based on the following theoretical description of nondiffusing singlet-born radical pairs, according to the formalism developed by P. Hore, in the high-field approximation.[43]

For each orientation of the molecule with respect to the external magnetic field **B**, without taking into account explicitly hyperfine interactions, which will be included in the inhomogeneous broadening of the absorption lines, the spin Hamiltonian of the radical pair may be written as

$$\hat{H} = \omega_A \hat{S}_{Az} + \omega_B \hat{S}_{Bz} - J(\hat{S}^2 - 1) + 1/2 D_{zz}(3\hat{S}_z^{\,2} - \hat{S}^2)$$

where $\hat{S}_{Az}$ and $\hat{S}_{Bz}$ are the z components of the electron spin angular momentum of the two radicals, $\hat{S}$ is the total electron spin angular momentum operator, J is the isotropic exchange interaction, ω_A and ω_B are the EPR frequencies of the two radicals in the absence of magnetic spin−spin interactions $\omega_{A,B} = g_{A,B}(\phi,\theta)\mu_B \hbar^{-1} B_0$, ϕ and θ denoting the angles defining the orientation of the magnetic field **B** with respect to the axis system of the g-tensors, and $D_{zz} = D(\cos^2 \xi - {}^1/_3)$, ξ being the angle between the dipolar axis and the magnetic field direction **B**. In this frame, the spin-correlated radical pair spectrum consists of two doublets in antiphase of equal amplitude, centered at the Larmor frequencies of the individual radicals forming the pair. The splitting of each doublet is due to the exchange contribution J and the magnetic dipolar contribution D_{zz}. The frequencies of the four spin-polarized EPR lines are

$$\omega_{12} = \omega_0 - \Omega - J + D_{zz}$$

$$\omega_{34} = \omega_0 - \Omega + J - D_{zz}$$

$$\omega_{13} = \omega_0 + \Omega - J + D_{zz}$$

$$\omega_{24} = \omega_0 + \Omega + J - D_{zz}$$

where

$$\omega_0 = (\omega_A + \omega_B)/2$$

and

$$\Omega^2 = (J + D_{zz}/2)^2 + Q^2$$

and

$$Q = (\omega_A - \omega_B)/2$$

While the TREPR spectra in frozen solution reflect the powder average over all possible orientations, the partially ordered spectra in the LC medium have been calculated introducing a Gaussian orientational distribution function for the molecular alignment axis relative to the director of the mesophase **L**. Assuming that triad **1** is characterized by a long molecular axis, as suggested by the optimized ground-state geometry and by the experiments in LC (Results section), the orientational distribution can be written as a function of only one angle, which describes the orientation of the molecular alignment axis with respect to **L**. The order parameter S, which characterizes the alignment of the molecule in the LC, may be written as

$$S = \frac{1}{2}\langle(3\cos^2 \alpha - 1)\rangle = \frac{\int f(\alpha)(3\cos^2 \alpha - 1)\, d\Omega}{\int f(\alpha)\, d\Omega}$$

where α is the deviation of the molecular axis orientation from **L** and $f(\alpha)$ is the Gaussian distribution describing the probability function for the deviation.

Simulations of the spin-polarized triplet spectra in 2-MeTHF were performed using a home-written FORTRAN program for a powder distribution of molecular orientations.

Results

TREPR in 2-MeTHF. Figure 2 shows the spin-polarized EPR spectrum 450 ns after the laser pulse of triad **1** in 2-MeTHF at 10 K. In the $g \cong 2$ region, the spectrum is dominated by narrow features, which can be attributed to a spin-correlated radical pair formed by photoinduced electron transfer. An enlargement of the radical pair spectral region is shown in the inset of Figure 2.

Two antiphase doublets are present in the spectrum, one being very weak in intensity. The different signal amplitudes are due to the different line widths of the two radicals forming the spin-correlated radical pair, as explained in the next section. The spectrum also exhibits broad spectral contributions, which are due to the presence of different triplet states. On the basis of the zero-field-splitting (ZFS) parameters, the broad signals are attributed to triplet states localized on the porphyrin and the fullerene moieties.[55−57] The porphyrin triplet resonates over a wider spectral range, about 900 G, than the fullerene triplet, about 100 G. The observed polarization pattern (aeaeae) of the fullerene triplet is typical for spin−orbit selective intersystem crossing (ISC) from the corresponding excited singlet state,[57] while the porphyrin triplet spectrum shows an unusual polarization pattern (eeeaaa) when compared to the one (eaeaea) reported for the powder spectrum of a randomly oriented porphyrin triplet state populated by ISC from the excited singlet state.[55] The ZFS parameters $|D|$ and $|E|$ and the relative population rates A_x, A_y, and A_z were derived from simulations of the randomly distributed triplet state spectra. The spectral parameters are the following: $|D| = 0.0099$ cm^{-1}, $|E| = 0.0012$ cm^{-1}, $A_x = 0.76$, $A_y = 0.23$, and $A_z = 0.01$ for the fullerene triplet and $|D| = 0.0364$ cm^{-1}, $|E| = 0.0077$ cm^{-1}, $A_x = 0.47$, $A_y = 0.52$, and $A_z = 0.01$ for the porphyrin triplet state.

The fullerene triplet signal decays 2 times faster in the triad than in the Me-fulleropyrrolidine model compound **2**, while the porphyrin triplet signal decays with the same kinetics as the corresponding model compound **3** (data not shown). Direct excitation of the fullerene moiety at the laser excitation wavelength (532 nm) cannot be avoided and may be responsible for the population of the fullerene triplet state in triad **1**. The unusual spin polarization of the porphyrin can be explained assuming a porphyrin triplet population arising mainly from energy transfer from the fullerene triplet state. This explanation is also in accord with the observed decrease in the fullerene triplet lifetime when it is linked to the porphyrin.

The antiphase doublets in the central part of the spectrum due to the charge-separated state are formed promptly, within the time resolution of the EPR spectrometer, and all the components decay with the same time constant of about 8 μs (inset of Figure 2). Thus, the radical pair lifetime at cryogenic temperatures is at least 8 μs, assuming that the intensity of the microwave field and spin−lattice relaxation rates are not affecting the kinetics, as expected under the experimental conditions used for EPR detection. However, the radical pair

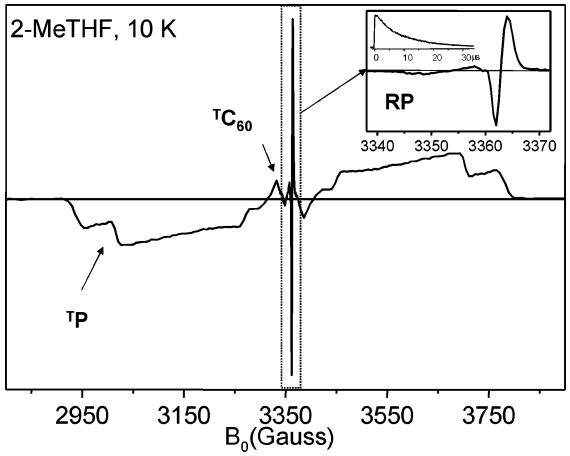

Figure 2. TREPR spectrum of TTF−P−C_{60} triad **1** in the isotropic glass of 2-MeTHF (T = 10 K) taken 450 ns after the laser pulse. The inset displays the expanded TREPR spectrum in the radical pair (RP) region and the time evolution at 3363 G, corresponding to the maximum of the RP positive peak.

recombination kinetics in 2-MeTHF at room temperature, as derived from time-resolved optical measurements,[36] are characterized by a TTF$^{\bullet+}$−P−$C_{60}^{\bullet-}$ lifetime of only 660 ns.

To assign the spin-polarized radical pair signal, simulations of the EPR spectrum have been performed in the framework of the spin-correlated radical pair mechanism.[43] Time-resolved optical studies of triad **1** in polar solvents at ambient temperatures have shown[36] that photoinduced electron transfer from the porphyrin first excited singlet state TTF−^{1}P−C_{60} yields an initial, short-lived (230 ps), charge-separated state TTF−P$^{\bullet+}$−$C_{60}^{\bullet-}$ (Figure 1). A charge-shift reaction yields the final charge-separated state TTF$^{\bullet+}$−P−$C_{60}^{\bullet-}$. In the TREPR experiments, the radical pair is generated from a singlet precursor, and the spin polarization likely arises in the secondary TTF$^{\bullet+}$−P−$C_{60}^{\bullet-}$ radical pair, since the lifetime of TTF−P$^{\bullet+}$−$C_{60}^{\bullet-}$ is expected to be too short to allow spin polarization to develop from spin dephasing. Indeed, no evidence for the presence of the primary radical pair has been found in the TREPR spectra, and the symmetry in the intensity of the antiphase doublets excludes any development of spin polarization on the TTF−P$^{\bullet+}$−$C_{60}^{\bullet-}$ radical pair and transfer to the TTF$^{\bullet+}$−P−$C_{60}^{\bullet-}$ radical pair.[58] The g-tensors and line widths used in the spectral simulations, reported in Table 1 together with all the simulation parameters, are in agreement with those of the corresponding tetrathiafulvalene and Me-fulleropyrrolidine radicals reported in the literature.[59−63] The dipolar interaction parameter ($D = -1.3$ G $= -12 \times 10^{-5}$ cm^{-1}) has been estimated in the point-dipole approximation for a center-to-center average distance between the two radicals of 28 Å, obtained from the optimized ground-state geometry of triad **1**, while the exchange interaction parameter J was varied to obtain the best-fit simulation of the spectrum (Figure 3, Table 1, and Discussion).

The good agreement between the experimental and calculated spectra allows definitive assignment of the radical pair spectrum to the secondary charge-separated state TTF$^{\bullet+}$−P−$C_{60}^{\bullet-}$. The two doublets belonging to the radical pair are not compatible with the reported g-factors for model porphyrin cations and anions and their large line widths.[64,65] Therefore, the radical pair EPR spectrum cannot arise from TTF$^{\bullet+}$−P$^{\bullet-}$−C_{60} or TTF−P$^{\bullet+}$−$C_{60}^{\bullet-}$.

It is interesting to note that the positive exchange interaction $J = +0.45 \pm 0.05$ G ($4.20 \times 10^{-5} \pm 0.5 \times 10^{-5}$ cm^{-1}) makes a substantial contribution to the total spin−spin coupling, despite the large separation between the two coupled radicals. A zero or negative value for the exchange interaction parameter is not compatible with the spin polarization pattern of the randomly distributed spectrum in 2-MeTHF glass because an opposite polarization would be produced.

TABLE 1: Spectral Parameters Used for the TTF$^{\bullet+}$−P−$C_{60}^{\bullet-}$ Radical Pair Spectra Simulation in 2-MeTHF Glass and in the Nematic Phase of the LC E−7 Reported in Figures 3 and 5, According to the Model Described in the Experimental Section[a]

g-tensor[b]

	g_{xx}	g_{yy}	g_{zz}	$\langle g \rangle$[c]
TTF$^{\bullet+}$	2.0090	2.0045	2.0015	2.0050
$C_{60}^{\bullet-}$	2.0008	2.0004	1.9993	2.0002

spin−spin coupling of TTF$^{\bullet+}$P$C_{60}^{\bullet-}$

D	-12×10^{-5} cm^{-1}
J	$+4.2 \times 10^{-5} \pm 0.5 \times 10^{-5}$ cm^{-1}

tensor orientation[d]

	α	β	γ
g-tensor of TTF$^{\bullet+}$	0°	70°	20°
g-tensor of $C_{60}^{\bullet-}$	0°	25°	0°
D-tensor of TTF$^{\bullet+}$P$C_{60}^{\bullet-}$	0°	0°	0°

$\Delta H_{1/2}$[e]

TTF$^{\bullet+}$	5.3 G
$C_{60}^{\bullet-}$	1.7 G

[a] The parameters are discussed in the text. [b] Estimated error: ±0.0005. [c] The isotropic g-value. [d] The tensor orientation expressed in terms of Euler angles are given for rotation about Z by α, Y' by β, and Z' by γ, in the fixed molecular frame with the Z direction along the long molecular axis (in E−7 || **L**). Estimated error: ±5°. [e] $\Delta H_{1/2}$ is the full line width at half-height. Uncertainty: ±5%.

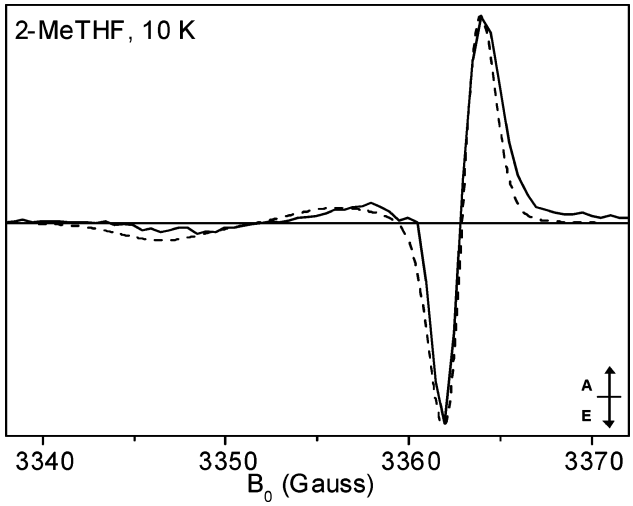

Figure 3. TREPR spectrum of the TTF$^{\bullet+}$−P−$C_{60}^{\bullet-}$ radical pair (—) taken 250 ns after the laser pulse in the isotropic glass of 2-MeTHF (T = 10 K) and the best-fit spectral simulation (- - -). The simulation parameters are reported in Table 1. A = absorption, E = emission.

TREPR in E−7. *Nematic Phase.* Figure 4 shows the spin-polarized TREPR spectrum of triad **1** taken 250 ns after the laser pulse, in the nematic phase of E−7 at ambient temperature. The TREPR spectrum exhibits narrow, polarized features that can be attributed to the TTF$^{\bullet+}$−P−$C_{60}^{\bullet-}$ radical pair. It also shows broad spectral contributions that are due to the presence of partially ordered triplet states, which are assigned to the porphyrin (all the emissive features at low field) and fullerene (absorptive features at low field close to the radical pair signal) moieties. The main contribution to the spectrum comes from the narrow radical pair signal (enlarged in the inset of Figure 4).

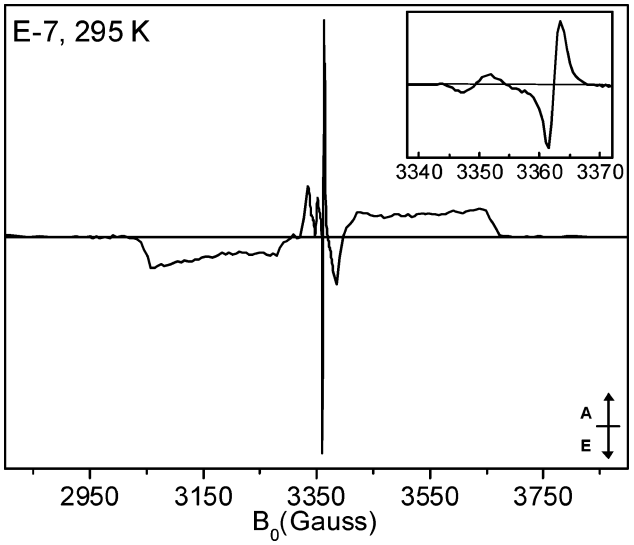

Figure 4. TREPR spectra of **1** in the nematic phase (**L** || **B**) of the LC E−7 (T = 295 K) taken 250 ns after the laser pulse. The inset displays the expanded TREPR spectrum in the radical pair region. A = absorption, E = emission.

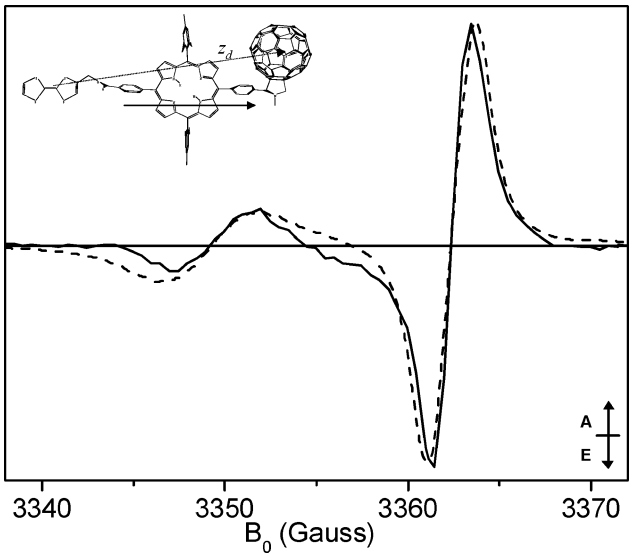

Figure 5. TREPR spectrum of the $TTF^{\bullet+}-P-C_{60}^{\bullet-}$ radical pair (—) taken 250 ns after the laser pulse in the nematic phase of the LC E−7 (295 K) and the best-fit spectral simulation (- - -). The simulation parameters are reported in Table 1. A = absorption, E = emission. In the molecular structure, the long axis direction and the dipolar vector z_d of $TTF^{\bullet+}-P-C_{60}^{\bullet-}$ are indicated.

Both of the antiphase doublets of the spin-correlated radical pair are clearly distinguishable. Charge separation is achieved in high quantum yield throughout the overall range of the nematic phase (up to 320 K). Even in the isotropic phase (up to 360 K), a spin-polarized radical pair signal has been detected (data not shown), and thermalization does not take place during the radical pair lifetime.

Simulation of the nematic phase experimental spectrum of triad **1** taken 250 ns after the laser pulse has been achieved. Figure 5 shows the TREPR experimental spectrum in the radical pair spectral region 250 ns after the laser pulse, together with the best-fit simulation. Parameters of the fitting are reported in Table 1.

For the simulation, the dipolar axis z_d is taken to be roughly parallel to the long axis of the molecule, as shown in Figure 5, and it is aligned with the LC director **L**, as discussed in the next section concerning the *crystalline phase*. The dipolar interaction ($D = -12 \times 10^{-5}$ cm^{-1}) has been taken as a fixed parameter, assuming an extended conformation as in the isotropic solvent. The J parameter obtained from the fitting procedure is in good agreement with the value obtained from the simulations of the spin-correlated radical pair in the 2-MeTHF glass. The g-tensors and line widths are those used for the simulations in isotropic solvent at 10 K. The $TTF^{\bullet+}$ g-tensor orientations are compatible with the extended conformation of the triad suggested by molecular modeling and reported in Figure 5. The largest g_{xx} component, which is directed along the long molecular axis of the TTF molecule, as determined by single-crystal EPR experiments performed on the BEDT−TTF radical cation,[60] is almost parallel to the alignment axis of the triad and therefore to the director **L** of the LC. On the basis of the simulation, it can be concluded that in the nematic phase of E−7 the radical pair observed by TREPR cannot arise either from the $TTF^{\bullet+}-P^{\bullet-}-C_{60}$ or from the $TTF-P^{\bullet+}-C_{60}^{\bullet-}$ charge-separated state, and definitive assignment to the secondary charge-separated state $TTF^{\bullet+}-P-C_{60}^{\bullet-}$ can be made. Moreover, the polarization pattern shows that the primary charge-separated state evolves rapidly into the secondary one without development of polarization.

In Figure 6, the time evolution of the radical pair portion of the spectrum is shown for the nematic phase of the LC at room temperature. The whole radical pair spectrum exhibits a strong polarization phase inversion with time, which is also clearly visible in the transient EPR signal corresponding to the high-field line of the most intense doublet of the $TTF^{\bullet+}-P-C_{60}^{\bullet-}$ radical pair (inset in Figure 6).

Since the spectral positions of the inverted doublets are maintained, it can be assumed that they describe the same radical pair state. The polarization phase inversion is clear evidence of the coexistence of singlet- and triplet-initiated routes for populating $TTF^{\bullet+}-P-C_{60}^{\bullet-}$ in this phase of the LC. No effect of microwave power has been observed on the relative intensity of the signals with opposite phase.

The initial, singlet-born radical pair decays rapidly, whereas the phase-inverted signal, corresponding to the triplet-born radical pair, is particularly long-lived, decaying with a time constant of ~ 7 μs. The triplet-born radical pair must arise from a triplet state of one of the chromophores (porphyrin or fullerene) of the triad. No definitive correlation between the appearance of the triplet radical pair and the decay of any precursor triplet state can be established because of the overlap of signals corresponding to the singlet-born and the triplet-born radical pairs and because of the instrumental time resolution, which precludes following the kinetics in the proper time window. However, both the porphyrin and the fullerene triplet state signal decay times in the nematic phase are altered compared to those for the respective model compounds measured under the same experimental conditions.

In the case of the fullerene model compound **2**, the triplet signal kinetics are characterized by fast relaxation rates that bring the initial spin polarization to a Boltzmann distribution, followed by an overall decay corresponding to the fullerene triplet lifetime. In triad **1**, the initial spin polarization does not have time to reach a Boltzmann distribution, and the EPR signal decays in a time window that is compatible with both triplet−triplet energy transfer to the porphyrin and triplet charge separation to form the final $^{T}(TTF^{\bullet+}-P-C_{60}^{\bullet-})$ radical pair. The porphyrin triplet EPR signal in **1** also decays more rapidly than that of the model porphyrin **3**, in the proper time window for formation of the triplet-born charge-separated state. Therefore,

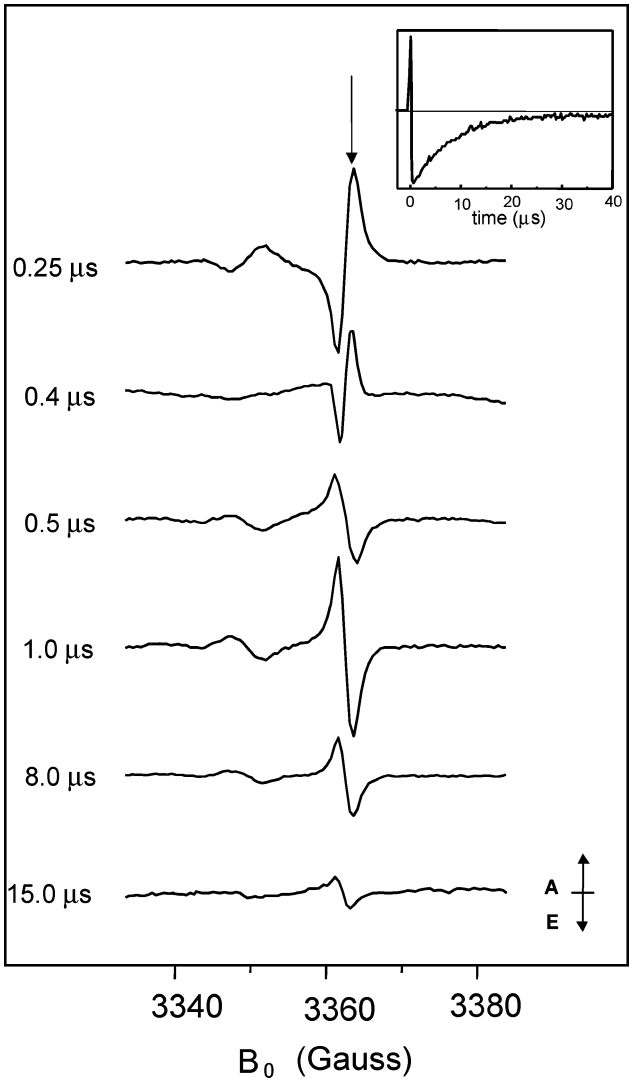

Figure 6. TREPR spectra of the $TTF^{\bullet+}-P-C_{60}^{\bullet-}$ radical pair in the nematic phase of the LC E−7 (295 K) at different delay times after the laser pulse as indicated. The inset displays the kinetic trace of $TTF^{\bullet+}-P-C_{60}^{\bullet-}$ at the field position indicated by an arrow. A = absorption, E = emission.

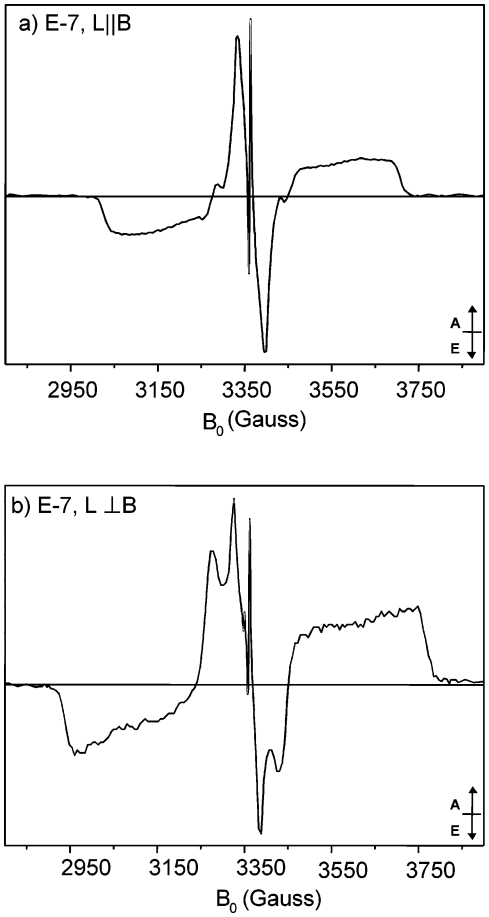

Figure 7. TREPR spectrum of **1** in the crystalline phase of LC E−7 (150 K) taken 250 ns after the laser pulse (a) at the parallel configuration between the LC director and the external magnetic field (**L** || **B**) and (b) at the perpendicular configuration (**L** ⊥ **B**). A = absorption, E = emission.

from a kinetic point of view, both triplet species are possible candidates for precursors that lead to triplet charge separation.

Crystalline Phase. Figure 7 shows the TREPR spectra of **1** in the crystalline phase of E−7 (T = 150K) taken 250 ns after the laser pulse. Spectra taken with the director **L** in the parallel (Figure 7a) and perpendicular (Figure 7b) configurations with respect to the external magnetic field are shown. In this phase, the narrow radical pair signal is no longer the dominant contribution to the spectra. Furthermore, the weaker doublet of the radical pair spectrum is not visible in the parallel configuration, being obscured by the fullerene triplet. It becomes visible in the perpendicular configuration due to reduction of the fullerene triplet contribution at the center of the spectrum.

The strong orientational dependence of the fullerene triplet signal indicates that the triad is well oriented in the nematic potential of the liquid crystal. A very similar orientation of the ZFS principal axes of the fullerene triplet, with respect to director **L**, has been obtained with an analogous C−P−C_{60} triad embedded in E−7.[22] This finding, together with the fact that a similar porphyrin bridge is featured in the two triads, leads to the conclusion that a similar overall orientation is reached by the two molecules in the liquid crystal. A detailed analysis of the orientational dependence of the triplet state spectra was performed for the C−P−C_{60} triad,[22] which led to the conclusion that the alignment axis corresponds to the long axis of the molecular triad. Therefore, as determined for the C−P−C_{60} triad, the preferred orientation of the TTF−P−C_{60} triad in the LC is again determined by the long molecular axis, joining the two phenyl groups connecting the TTF and C_{60} moieties (Figure 5). The orientation dependence of the partially ordered spectrum of the porphyrin triplet of **1** in the crystalline phase of E−7 at 150 K is also consistent with this orientation. More uncertainty concerns the relative conformation of the TTF moiety with respect to the porphyrin and fullerene moieties in the triad, because, unlike the C−P−C_{60} triad, no triplet state localized in the donor molecule helps in this case to determine the preferential conformation. However, both the molecular modeling and the *g*-tensor orientation of the $TTF^{\bullet+}$ radical in the magnetic field as determined by the simulation of the radical pair spectrum (Table 1) seem to suggest the extended conformation reported in Figure 5.

It will be noted that no phase inversion of the polarization pattern of the radical pair is produced upon rotation of the sample from the parallel to the perpendicular configuration (Figure 7). This is relevant to the spectral simulations for the nematic phase discussed earlier. A smaller value for the exchange integral J than the one reported, which could in principle be compensated for in the simulations by a larger value for the dipolar parameter, is not compatible with the invariance of the phase of the experimental spectrum when going from an

L || **B** to an **L** ⊥ **B** configuration in the crystalline phase. As predicted by the correlated radical pair sign rule, inversion of polarization would be expected in the case where the dipolar interaction is the main or only contribution to the splitting of the antiphase components of each EPR doublet.[43]

In the crystalline phase, spectra taken at different times show no phase inversion as a function of time and therefore no evidence for formation of a triplet-born charge-separated state such as that observed in the nematic phase. The singlet-born radical pair $TTF^{\bullet+}-P-C_{60}^{\bullet-}$ has a lifetime of ∼1.4 μs. In addition, no correlation between the decay of the radical pair and the growth of either the porphyrin or the fullerene triplet EPR signals has been found, consistent with the results of the previous optical spectroscopic investigation of triad **1** in 2-MeTHF solvent, where no recombination to a triplet state was observed.[36] Moreover, neither the porphyrin nor the fullerene triplet show the characteristic spin polarization derived from charge recombination of a radical pair with a singlet precursor.[43] The partially ordered TREPR spectrum of the fullerene triplet state is instead characterized by the polarization pattern produced by spin−orbit selective ISC from the corresponding singlet state,[57] as demonstrated by spectral simulations (not shown). As mentioned in the case of the 2-MeTHF glass, the partially ordered porphyrin triplet spectrum is characterized by an unusual polarization, indicating that this triplet is produced by energy transfer from the fullerene triplet state.

Discussion

2-MeTHF Glass. The TREPR studies of triad **1** in the isotropic 2-MeTHF glass at low temperatures have shown that the charge-separation processes that occur at ambient temperatures in this solvent also occur in the glass. Excitation of the porphyrin yields $TTF-{}^1P-C_{60}$, which decays by photoinduced electron transfer to yield $TTF-P^{\bullet+}-C_{60}^{\bullet-}$, which evolves by a charge-shift reaction to $TTF^{\bullet+}-P-C_{60}^{\bullet-}$. It is interesting to note that charge separation is still active in the glass, where solvent motions are restricted, solvent reorganization energies are reduced, and the charge-separated states are destabilized due to the inability of solvent molecules to solvate them fully through solvent reorganization. The occurrence of photoinduced charge separation in high yield in glasses at temperatures down to 8 K has also been observed in $C-P-C_{60}$ triads.[9,16,17,21,22] Such behavior is not observed in similar systems wherein the fullerene is replaced by quinone electron acceptors, but photoinduced electron transfer at cryogenic temperatures is characteristic of photosynthetic reaction centers. The fact that photoinduced electron transfer in the $C-P-C_{60}$ and $TTF-P-C_{60}$ triads does not cease at low temperatures when the solvent becomes glassy may be ascribed to several effects. The fullerene and porphyrin moieties both have relatively low internal reorganization energies and also low solvent reorganization energies. In addition, the radical ions of fullerenes are much less sensitive to solvent dielectric stabilization effects than are those of quinones. Because of these effects, photoinduced electron-transfer reactions that are only moderately exergonic at room temperature in polar solvents are still thermodynamically and kinetically viable at low temperatures in media with low dielectric constants.

Triad **1** was designed in such a way that, based on electrochemical measurements in polar solvents at ambient temperatures, no triplet state lies at a lower energy than the final charge-separated state $TTF^{\bullet+}-P-C_{60}^{\bullet-}$. This precludes the radical pair recombination to form triplet states that has been observed in analogous $C-P-C_{60}$ molecules and in natural photosynthesis. The TREPR measurements in 2-MeTHF glass (and all the other phases of LC investigated here) show that even when triplet states have been detected their polarization patterns are not those characteristic of the radical pair recombination mechanism.

The lifetime of $TTF^{\bullet+}-P-C_{60}^{\bullet-}$ is ∼8 μs in the isotropic glass, whereas it is only 660 ns in the liquid solvent at room temperature. This increase in lifetime is consistent with a reaction in the inverted region of the Marcus−Hush relationship, which describes the dependence of the electron-transfer rate constant on free energy change. The $TTF^{\bullet+}-P-C_{60}^{\bullet-}$ state is destabilized when the solvent becomes glassy, and solvent motions that would stabilize the charge-separated state are reduced or precluded. The effect is mainly due to the presence of $TTF^{\bullet+}$ since, as said above, the fullerene radical anion has relatively low internal and solvent reorganization energies. This moves the charge recombination reaction farther into the inverted region, leading to slower charge recombination. A decrease in solvent reorganization energy upon freezing also moves the recombination reaction farther into the inverted region.

Liquid Crystal. The use of the anisotropic liquid crystalline solvent for the TREPR studies permitted the investigation of the role of ordered media in controlling ET reaction rates. In addition, it was possible to study ET in the various phases of the solvent. The TREPR results demonstrate that there is a high degree of ordering of the triad molecules induced by the nematic potential. Simulation of the spectra in the nematic phase permitted derivation the relevant spectral parameters. In particular, this made it possible to extract the value of the exchange interaction J between the TTF radical cation and the C_{60} radical anion in $TTF^{\bullet+}-P-C_{60}^{\bullet-}$. This interaction is related to the electronic coupling matrix element V between the initial and final states in the charge recombination of $TTF^{\bullet+}-P-C_{60}^{\bullet-}$.[50−53] According to Marcus−Hush theory, the electron-transfer rate is proportional to V^2.[66] In the simulation, it was possible to restrict the range of possible values for J due to the absence of any effect on the radical pair spectra when going from the parallel (**L** || **B**) to the perpendicular (**L** ⊥ **B**) configurations of the LC in crystalline phase. The value obtained for J, 4.20×10^{-5} cm^{-1}, is significant, given the large spatial separation of the radical ions. If the exchange interaction depended exponentially on this separation, then one would expect an interaction parameter that is orders of magnitude smaller.[67] The value measured is consistent with the involvement of the porphyrin ring interposed between the TTF and the fullerene moieties via superexchange interactions. Since the dipolar interaction D used in the simulation is derived in the point-dipole approximation and could be affected by an error due to the large molecular size of both donor and acceptor moieties compared to the center-to-center distance, we have also calculated the spectra for minimum (20 Å) and maximum distances (33 Å) between the TTF and the *N*-methylfulleropyrrolidine molecules. A $D_{MAX} = -27 \times 10^{-5}$ cm^{-1} is not compatible with the experimental observations. To avoid phase inversion from the parallel to the perpendicular configuration corresponding to this value for the dipolar parameter, the exchange parameter should exceed 5.6×10^{-5} cm^{-1}, but the combination of the dipolar and exchange interaction parameters produces too large a splitting of the EPR doublets that is not compatible with the experimental spectra. This is true for all values of the dipolar parameter exceeding -13×10^{-5} cm^{-1}. For $D = -13 \times 10^{-5}$ cm^{-1}, a J parameter of 4.2×10^{-5} cm^{-1} is still compatible with the splitting of the radical pair lines. However, values down to $D_{MIN} = -6.4 \times 10^{-5}$ cm^{-1} corresponding to the largest edge-to edge distance

are still compatible with the J parameter within the confidence interval of $+4.2 \times 10^{-5} \pm 0.5 \times 10^{-5}$ cm^{-1} as obtained in the best-fit simulation with a D value (-12×10^{-5} cm^{-1}) calculated for the center-to-center distance (28 Å). We can therefore assess that the variation of the dipolar interaction in the range of acceptable values is not affecting the output value of the J parameter.

Triplet States. Porphyrin and fullerene triplet states were detected by TREPR in all solvents investigated. The spin polarization patterns of these triplets demonstrate that they do not arise from the recombination of radical pair states (as observed in related carotene−porphyrin−fullerene triads). The fullerene triplet arises from intersystem crossing from the fullerene singlet state. This singlet state is produced by direct excitation of the fullerene or by energy transfer from the porphyrin. Thus, photoinduced electron transfer from TTF−P−^{1}C$_{60}$ to yield TTF−P$^{\bullet+}$−C$_{60}^{\bullet-}$, although it may occur, is too slow to effectively eliminate ISC. The spin polarization of the porphyrin triplet state shows that a majority of this triplet forms via triplet−triplet energy transfer from the more energetic fullerene triplet. Such energy transfer has been observed in closely related molecules.[19] This is reasonable, as in fluid 2-MeTHF at ambient temperatures, the lifetime of the porphyrin first excited singlet state of **1** is only 25 ps, precluding a significant yield of TTF−^{3}P−C$_{60}$ by direct ISC.

A very interesting feature of the photochemistry of **1** in the nematic phase of E−7 is the fact that final TTF$^{\bullet+}$−P−C$_{60}^{\bullet-}$ states are formed from both singlet and triplet precursors. Charge separation from a triplet is not observed in the other phases. Two routes for formation of the triplet-born radical pair may be envisioned. One of these is direct electron transfer either from the porphyrin triplet to the fullerene or from the porphyrin to the fullerene triplet, generating ^{T}[TTF−P$^{\bullet+}$−C$_{60}^{\bullet-}$], which then evolves by charge shift to ^{T}[TTF$^{\bullet+}$−P−C$_{60}^{\bullet-}$]. This is analogous to the charge-separation route from the porphyrin excited singlet state. However, Figure 1 suggests that such an electron transfer would be endergonic by ∼0.1−0.2 eV. The energies of the charge-separated states shown in Figure 1 are based on oxidation and reduction potentials of triad **1** and model compounds measured by cyclic voltammetry in a polar solvent, benzonitrile ($\epsilon = 25.2$).[36] The triplet energies are those reported for model compounds. On the basis of simply dielectric constant considerations, the redox potentials in E−7 ($\epsilon = 19.6$) are expected to be similar, and the energies of the charge-separated states should be similar or even a bit higher. Thus, if the triplet-born radical pair is derived from the fullerene or porphyrin triplet states via the stepwise electron-transfer mechanism, then the energies of at least one triplet state and one of the possible intermediate charge-separated states must be similar or inverted relative to the energies shown in Figure 1. Slightly endergonic electron transfer is compatible with time constants in the hundreds of nanoseconds range. Observations consistent with this hypothesis are the fact that triplet-born radical pairs exist and the fact that the lifetimes of the porphyrin and fullerene triplet states of **1** in the nematic phase are shortened relative to those of model systems **2** and **3**. Triplet-born radical pairs are not observed in the crystalline phase of E−7. This is consistent with the mechanism under discussion in that the crystalline phase would be less mobile than the nematic phase and thus less able to stabilize a charge-separated state. This effect could lead to an energy of the initially formed charge-separated state that is high enough so that photoinduced ET from a triplet state is no longer possible at the temperatures investigated.

An alternative possibility for formation of the triplet-born radical pair TTF$^{\bullet+}$−P−C$_{60}^{\bullet-}$ is direct photoinduced electron transfer from TTF to the fullerene triplet state via a superexchange mechanism involving the porphyrin. This possibility is thermodynamically reasonable. In addition, the nonzero value measured for J demonstrates that a significant electronic coupling between the radical ions, mediated by the porphyrin, does exist. Presumably, a similar coupling between the ground-state TTF and ^{3}C$_{60}$ also exists. Such transfer in the singlet manifold is expected to be much slower than the two-step mechanism, as the electronic coupling is much weaker. However, in the triplet manifold, the lifetimes of the excited states are much longer, allowing slower reactions to occur with a significant quantum yield.

An interesting consequence of the operation of two concurrent pathways for the formation of TTF$^{\bullet+}$−P−C$_{60}^{\bullet-}$ in the nematic phase at ambient temperatures is the large difference in lifetimes of the charge-separated states in the high magnetic field. The singlet-born radical pair decays in less than 1 μs, whereas the triplet-born radical pair persists for ∼7 μs. The lifetime of the singlet-born pair is roughly similar to that of the radical pair formed in the isotropic, solution phase of 2-MeTHF. The spin-correlated radical pair can be described, in the presence of an external magnetic field, in terms of four spin states, two pure triplet states, T_{-1} and T_{+1}, and two states that are combinations of S, T_0.[43] In the absence of the external magnetic field, all four spin sublevels of the radical pair have some singlet character and are of nearly identical energies. All four states would rapidly equilibrate during the lifetime of the charge-separated state, making the decay to the ground state fast and comparable to that of singlet-born radical pair.[68] In the presence of the magnetic field of the EPR spectrometer, the T_{-1} and T_{+1} states of the biradical are energetically split from the S and T_0 states. Under these conditions, the singlet-born radical pair, which is initially populated only in the S and T_0 states, cannot equilibrate with the T_{-1} and T_{+1} states during its lifetime. Therefore, the state still decays on the hundreds of nanoseconds time scale. However, the fraction of the triplet-born radical pairs that form in the T_{-1} and T_{+1} states cannot equilibrate fast with the S state, direct recombination to the ground state is spin forbidden, and there are no lower-lying triplet states available. Thus, the lifetime of the triplet-born radical pair is considerably extended.

Conclusions

Photoinduced electron transfer in TTF−P−C$_{60}$ triad **1** to form a long-lived charge-separated state TTF$^{\bullet+}$−P−C$_{60}^{\bullet-}$ has been investigated by TREPR spectroscopy. In an isotropic glass of 2-MeTHF at 10 K, the charge separation and recombination processes have essentially the same nature as those previously reported for this solvent at ambient temperatures. Photoinduced electron transfer from TTF−^{1}P−C$_{60}$ yields an intermediate, TTF−P$^{\bullet+}$−C$_{60}^{\bullet-}$, and charge shift yields the final state. However, the lifetime of TTF$^{\bullet+}$−P−C$_{60}^{\bullet-}$ in the glass, ∼8 μs, is considerably longer than that observed in fluid solution at ambient temperatures (660 ns). The assignment of an excited singlet state precursor for charge separation, made on the basis of optical spectroscopic measurements in fluid solution, was verified by the observation of the expected spin polarization of the radical pair. The triad was also studied in the liquid crystal E−7. At low temperature in the crystalline phase, TTF$^{\bullet+}$−P−C$_{60}^{\bullet-}$ was formed by a mechanism similar to that observed in the isotropic phase. However, the molecule was strongly oriented in the LC and the magnetic field, with the long axis of the molecule lying approximately along the director of the LC. In the nematic phase of E−7 at ambient temperatures,

a radical pair state with a lifetime of less than 1 μs forms, as occurs in 2-MeTHF at ambient temperatures. In addition, a long-lived ($\sim$7 μs) $TTF^{\bullet+}-P-C_{60}^{\bullet-}$ state is observed. This interesting species is ascribed to the triplet biradical formed by electron transfer involving either the fullerene or the porphyrin triplet state. The long lifetime is ascribed to the strong magnetic field, which prevents the charge-separated state from equilibrating with the singlet biradical state.

Long-lived charge separation is desirable for possible solar energy conversion or optoelectronic applications.

Acknowledgment. This work was supported by the PRIN (Project No. 2002031443), the CNR (Project No. CNRG004079), and the U.S. National Science Foundation (Grant No. CHE-0352599).

References and Notes

(1) Gust, D.; Moore, T. A. *Adv. Photochem.* **1991**, *16*, 1−65.
(2) Wasielewski, M. R. *Chem. Rev.* **1992**, *92*, 435−461.
(3) Kurreck, H.; Huber, M. *Angew. Chem., Int. Ed. Engl.* **1995**, *34*, 849−866.
(4) Gust, D.; Moore, T. A.; Moore, A. L. *Pure Appl. Chem.* **1998**, *70*, 2189−2200.
(5) Gust, D.; Moore, T. A. Intramolecular Photinduced Electron-Transfer Reactions of Porphyrins. In *The Porphyrin Handbook*; Kadish, K. M., Smith, K. M., Guilard, R., Eds.; Academic Press: New York, 2000; Vol. 8, pp 153−190.
(6) Gust, D.; Moore, T. A.; Moore, A. L. *Acc. Chem. Res.* **2001**, *34*, 40−48.
(7) Moore, T. A.; Moore, A. L.; Gust, D. *Philos. Trans. R. Soc. London, Ser. B* **2002**, *357*, 1481−1498.
(8) Larsson, S.; Klimkãns, A.; Rodriguez-Monge, L.; Duškesas, G. *THEOCHEM* **1998**, *425*, 155−159.
(9) Kuciauskas, D.; Liddell, P. A.; Lin, S.; Stone, S. G.; Moore, A. L.; Moore, T. A.; Gust, D. *J. Phys. Chem. B* **2000**, *104*, 4307−4321.
(10) Imahori, H.; Yamada, H.; Guldi, D. M.; Endo, Y.; Shimomura, A.; Kundu, S.; Yamada, K.; Okada, T.; Sakata, Y.; Fukuzumi, S. *Angew. Chem., Int. Ed.* **2002**, *41*, 2344−2347.
(11) Guldi, D. M.; Luo, C.; Kotov, N. A.; Da Ros, T.; Bosi, S.; Prato, M. *J. Phys. Chem. B* **2003**, *107*, 7293−7298.
(12) Liddell, P. A.; Sumida, J. P.; Machperson, A. N.; Noss, L.; Seely, G. R.; Clark, K. N.; Moore, A. L.; Moore, T. A.; Gust, D. *Photochem. Photobiol.* **1994**, *60*, 537−541.
(13) Imahori, H.; Sakata, Y. *Adv. Mater.* **1997**, *9*, 537−546.
(14) Meijer, M. D.; van Klink, G. P. M.; van Koten, G. *Coord. Chem. Rev.* **2002**, *230*, 141−163.
(15) Guldi, D. M. *Pure Appl. Chem.* **2003**, *75*, 1069−1075.
(16) Liddell, P. A.; Kuciauskas, D.; Sumida, J. P.; Nash, B.; Nguyen, D.; Moore, A. L.; Moore, T. A.; Gust, D. *J. Am. Chem. Soc.* **1997**, *119*, 1400−1405.
(17) Carbonera, D.; Di Valentin, M.; Corvaja, C.; Agostini, G.; Giacometti, G.; Liddell, P. A.; Kuciauskas, D.; Moore, A. L.; Moore, T. A.; Gust, D. *J. Am. Chem. Soc.* **1998**, *120*, 4398−4405.
(18) Kuciauskas, D.; Liddell, P. A.; Moore, A. L.; Moore, T. A.; Gust, D. *J. Am. Chem. Soc.* **1998**, *120*, 10880−10886.
(19) Gust, D.; Moore, T. A.; Moore, A. L.; Kuciauskas, D.; Liddell, P. A.; Halbert, B. D. *J. Photochem. Photobiol. B* **1998**, *43*, 209−216.
(20) Bahr, J. L.; Kuciauskas, D.; Liddell, P. A.; Moore, A. L.; Moore, T. A.; Gust, D. *Photochem. Photobiol.* **2000**, *72*, 598−611.
(21) Di Valentin, M.; Bisol, A.; Giacometti, G.; Carbonera, D.; Agostini, G.; Liddell, P. A.; Moore, A. L.; Moore, T. A.; Gust, D. *Mol. Cryst. Liq. Cryst.* **2003**, *394*, 19−30.
(22) Di Valentin, M.; Bisol, A.; Agostini, G.; Fuhs, M.; Liddell, P. A.; Moore, A. L.; Moore, T. A.; Gust, D.; Carbonera, D. *J. Am. Chem. Soc.* **2004**, *126*, 17074−17086.
(23) Rutherford, A. W.; Paterson, D. R.; Mullet, J. E. *Biochim. Biophys. Acta* **1981**, *635*, 205−214.
(24) McGann, W. J.; Frank, H. A. *Chem. Phys. Lett.* **1985**, *121*, 253−261.
(25) Prato, M.; Maggini, M.; Giacometti, C.; Scorrano, G.; Sandonà, G.; Farnia, G. *Tetrahedron* **1996**, *52*, 5221−5234.
(26) Boulle, C.; Rabreau, J. M.; Hudhomme, P.; Cariou, M.; Jubault, M.; Gorgues, A.; Orduna, J.; Garín, J. *Tetrahedron Lett.* **1997**, *38*, 3909−3910.
(27) Llacay, J.; Veciana, J.; Vidal-Gancedo, J.; Bourdelande, J. L.; Gonzalez-Moreno, R.; Rovira, C. *J. Org. Chem.* **1998**, *63*, 5201−5210.
(28) Bryce, M. R. *Adv. Mater.* **1999**, *11*, 11−23.
(29) Guldi, D. M.; González, S.; Martín, N.; Antón, A.; Garín, J.; Orduna, J. *J. Org. Chem.* **2000**, *65*, 1978−1983.
(30) Martín, N.; Sánchez, L.; Herranz, M. A.; Guldi, D. M. *J. Phys. Chem. A* **2000**, *104*, 4648−4657.
(31) Allard, E.; Cousseau, J.; Ordúna, J.; Garín, J.; Luo, H.; Araki, Y.; Ito, O. *Phys. Chem. Chem. Phys.* **2002**, *4*, 5944−5951.
(32) Kreher, D.; Hudhomme, P.; Gorgues, A.; Luo, H.; Araki, Y.; Ito, O. *Phys. Chem. Chem. Phys.* **2003**, *5*, 4583−4592.
(33) Segura, M.; Sanchez, L.; de Mendoza, J.; Martin, N.; Guldi, D. M. *J. Am. Chem. Soc.* **2003**, *125*, 15093−15100.
(34) Williams, R. M.; Zwier, J. M.; Verhoeven, J. W. *J. Am. Chem. Soc.* **1995**, *117*, 4093−4099.
(35) Pou-Amérigo, R.; Ortí, E.; Merchán, M.; Rubio, M.; Viruela, P. M. *J. Phys. Chem. A* **2002**, *106*, 631−640.
(36) Liddell, P. A.; Kodis, G.; de la Garza, L.; Bahr, J. L.; Moore, A. L.; Moore, T. A.; Gust, D. *Helv. Chim. Acta* **2001**, *84*, 2765−2783.
(37) Kodis, G.; Liddell, P. A.; de la Garza, L.; Moore, A. L.; Moore, T. A.; Gust, D. *J. Mater. Chem.* **2002**, *12*, 2100−2108.
(38) Levanon, H.; Hasharoni, K. *Prog. React. Kinet.* **1995**, *20*, 309−346.
(39) Levanon, H.; Möbius, K. *Annu. Rev. Biophys. Biomol. Struct.* **1997**, *26*, 495−540.
(40) Steinberg-Yfrach, G.; Liddell, P. A.; Hung, S.-C.; Moore, A. L.; Gust, D.; Moore, T. A. *Nature* **1997**, *385*, 239−241.
(41) Steinberg-Yfrach, G.; Rigaud, J. L.; Durantini, E. N.; Moore, A. L.; Gust, D.; Moore, T. A. *Nature* **1998**, *392*, 479−482.
(42) Bennett, I. M.; Vanegas Farfano, H. M.; Bogani, F.; Primak, A.; Liddell, P. A.; Otero, L.; Sereno, L.; Silber, J. J.; Moore, A. L.; Moore, T. A.; Gust, D. *Nature* **2002**, *420*, 398−401.
(43) Hore, P. J. Analysis of Polarized EPR Spectra. In *Advanced EPR: Applications in Biology and Biochemistry*; Hoff, A. J., Ed.; Elsevier Science Publishers: Amsterdam, The Netherlands, 1989; Chapter 12, pp 405−440.
(44) Hasharoni, K.; Levanon, H. *J. Phys. Chem.* **1995**, *99*, 4875−4878.
(45) Hasharoni, K.; Levanon, H.; von Gersdorff, J.; Kurreck, H.; Möbius, K. *J. Chem. Phys.* **1993**, *98*, 2916−2926.
(46) Shaakov, S.; Galili, T.; Stavitski, E.; Levanon, H.; Lukas, A.; Wasielewski, M. R. *J. Am. Chem. Soc.* **2003**, *125*, 6563−6572.
(47) Levanon, H.; Galili, T.; Regev, A.; Wiederrecht, G. P.; Svec, W. A.; Wasielewski, M. R. *J. Am. Chem. Soc.* **1998**, *120*, 6366−6373.
(48) Fuhs, M.; Elger, G.; Osintsev, A.; Popov, A.; Kurreck, H.; Möbius, K. *Mol. Phys.* **2000**, *98*, 1025−1040.
(49) Heinen, U.; Berthold, T.; Kothe, G.; Stavitski, E.; Galili, T.; Levanon, H.; Wiederrecht, G. P.; Wasielewski, M. R. *J. Phys. Chem. A* **2002**, *106*, 1933−1937.
(50) Anderson, P. W. *Phys. Rev.* **1959**, *115*, 2−13.
(51) Hoff, A. J.; Deisenhofer, J. *Phys. Rep.* **1997**, *287*, 195−208.
(52) Calvo, R.; Abresch, E. C.; Bittl, R.; Feher, G.; Hofbauer, W.; Isaacson, R. A.; Lubitz, W.; Okamura, M. Y.; Paddock, M. L. *J. Am. Chem. Soc.* **2000**, *122*, 7327−7341.
(53) Weiss, E. A.; Ratner, M. A.; Wasielewski, M. R. *J. Phys. Chem. A* **2003**, *107*, 3639−3647.
(54) Gonen, O.; Levanon, H. *J. Chem. Phys.* **1985**, *89*, 1637−1643.
(55) Gonen, O.; Levanon, H. *J. Chem. Phys.* **1986**, *84*, 4132−4141.
(56) Agostini, G.; Corvaja, C.; Pasimeni, L. *Chem. Phys.* **1996**, *202*, 349−356.
(57) Pasimeni, L.; Segre, U.; Ruzzi, M.; Maggini, M.; Prato, M.; Kordatos, K. *J. Phys. Chem. B* **1999**, *103*, 11275−11281.
(58) Morris, A. L.; Norris, J. R.; Thurnauer, M. C. An Extended Model for Electron Spin Polarization in Photosynthetic Bacteria. In *Reaction Centers of Photosynthetic Bacteria*; Michel-Beyerle, M. E., Ed.; Springer Series in Biophysics 6; Springer-Verlag: Berlin, Germany, 1990; pp 423−435.
(59) Walsh, W. M. J.; Rupp, L. W.; Wudl, F.; Kaplan, M. L.; Schfer, D. E.; Thomas, G. A.; Gemmer, R. *Solid State Commun.* **1980**, *33*, 413−416.
(60) Sugano, T.; Saito, G.; Kinoshita, M. *Phys. Rev. B* **1986**, *34*, 117−125.
(61) Coffen, D. L.; Chamber, J. Q.; Williams, D. R.; Garrett, P. E.; Canfield, N. D. *J. Am. Chem. Soc.* **1971**, *9*, 2258−2268.
(62) Brustolon, M.; Zoleo, A.; Agostini, G.; Maggini, M. *J. Phys. Chem. A* **1998**, *102*, 6331−6339.
(63) Zoleo, A.; Maniero, A. L.; Prato, M.; Severin, M. G.; Brunel, L. C.; Kordatos, K.; Brustolon, M. *J. Phys. Chem. A* **2000**, *104*, 9853−9863.
(64) Fajer, J.; Davis, M. S. Electron Spin Resonance of Porphyrin π Cations and Anions. In *The Porphyrins*; Dolphin, D., Ed.; Academic Press: New York, 1978; Vol. 4, pp 197−236.
(65) Seth, J.; Bocian, D. F. *J. Am. Chem. Soc.* **1994**, *116*, 143−153.
(66) Marcus, R. A.; Sutin, N. *Biochim. Biophys. Acta* **1985**, *811*, 265−322.
(67) de Kanter, F. J. J.; den Hollander, J. A.; Huizer, A. H.; Kaptein, R. *Mol. Phys.* **1977**, *34*, 857.
(68) van Dijk, B.; Carpenter, J. K. H.; Hoff, A. J.; Hore, P. J. *J. Phys. Chem. B* **1998**, *102*, 464−472.